

AD-A034 649

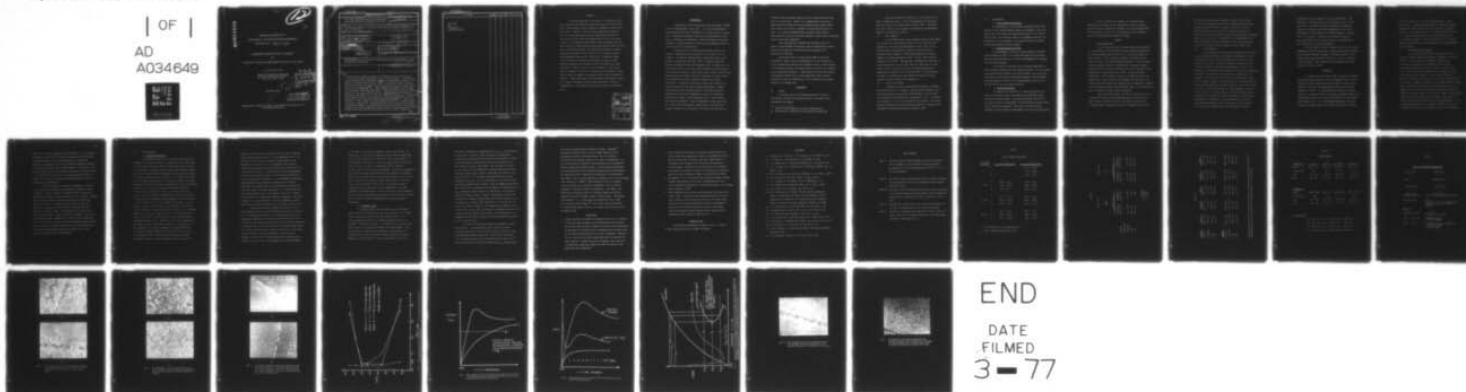
RENSSELAER POLYTECHNIC INST TROY N Y DEPT OF MATERIA--ETC F/G 11/6
MICROSTRUCTURE STUDY OF THE EFFECT OF TITANIUM IN THE AGING TRE--ETC(U)
DEC 76 C CHEN, & JUDD N00014-75-C-0504

UNCLASSIFIED

TR-8

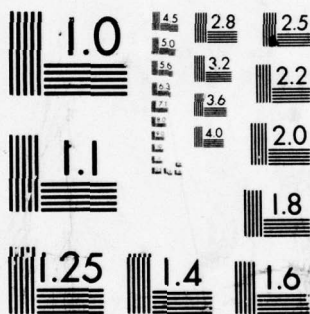
NL

| OF |
AD
A034649



END

DATE
FILMED
3-77



MICROCOPY RESOLUTION TEST CHART
NATIONAL BUREAU OF STANDARDS-1963-A

ADA034649

12

8

TECHNICAL REPORT NO. 8

SPONSORED BY THE OFFICE OF NAVAL RESEARCH

CONTRACT NO. N00014-75-C-0504

302-125

MICROSTRUCTURE STUDY ON THE EFFECT
OF
TITANIUM IN THE AGING TREATMENT OF AN Al-Zn-Mg ALLOY

C. Chen and G. Judd

Materials Engineering Department
Rensselaer Polytechnic Institute
Troy, New York 12181

DDC
RECEIVED
JAN 19 1977

December 1976

147308-A
DISTRIBUTION STATEMENT A
Approved for public release;
Distribution Unlimited

Reproduction in whole or in part is permitted for any purpose of the
United States Government

unclassified

Security Classification

DOCUMENT CONTROL DATA - R & D

(Security classification of title, body of abstract and indexing annotation must be entered when the overall report is classified)

1. ORIGINATING ACTIVITY (Corporate author) Gary Judd, Materials Engineering Department Rensselaer Polytechnic Institute, Troy, NY		2a. REPORT SECURITY CLASSIFICATION unclassified	
3. REPORT TITLE ⑥ Microstructure Study on the Effect of Titanium in the Aging Treatment of an Al-Zn-Mg Alloy.		2b. GROUP	
4. DESCRIPTIVE NOTES (Type of report and inclusive dates)			
5. AUTHOR(S) (First name, middle initial, last name) ⑩ Chun/Chen and Gary/Judd			
6. REPORT DATE ⑪ Dec 76		7a. TOTAL NO. OF PAGES 32	7b. NO. OF REFS 18
8a. CONTRACT OR GRANT NO. ⑮ N00014-75-C-0504		9a. ORIGINATOR'S REPORT NUMBER(S) ⑨ Technical Report #8	
c. PROJECT NO. ⑫ 35 p.		9b. OTHER REPORT NO(S) (Any other numbers that may be assigned this report)	
10. DISTRIBUTION STATEMENT Reproduction in whole or in part is permitted for any purpose of the United States Government.			
11. SUPPLEMENTARY NOTES		12. SPONSORING MILITARY AGENCY Approved for public release; DISSEM Unlimited	
13. ABSTRACT A study has been made on the effect of Ti additions on the microstructure in two stage and single stage aging of an Al-5 Zn-2 Mg alloy. The influence of aging treatment was examined for alloys with and without Ti addition. The alloys were solution heat treated at 510°C, air cooled then aged at various temperatures below the G. P. zone solvus for short times before aging above the G. P. zone solvus at 200°C. The Ti addition alloy yields a small precipitate free zone (PFZ) (0.3 μ) and a higher density of precipitate near the edge of the PFZ than in the mid-grain region. The ternary alloy without Ti addition produces a wide range of PFZ sizes (0.4 to 4 μ) depending upon the aging temperature below the G. P. zone solvus. Significant changes in the morphology of the matrix precipitate, the amount of grain boundary precipitate, and the width of PFZ were observed in single stage aging at 200°C as a result of the Ti addition. These results could be explained in terms of Ti interacting with vacancies or solute atoms, causing the changes in the vacancy/and/or solute concentration profiles. A model based upon solute and vacancy/concentrations coupled with a time at temperature effect has been developed to allow the interpretation of the observed two-stage aging results in an Al-Zn-Mg alloy.			

DD FORM 1473

unclassified

Security Classification

302 125

unclassified

Security Classification

14	KEY WORDS	LINK A		LINK B		LINK C	
		ROLE	WT	ROLE	WT	ROLE	WT
	Al-Zn-Mg PFZ Precipitation Titanium additions						

unclassified

Security Classification

ABSTRACT

A study has been made on the effect of Ti additions on the microstructure in two stage and single stage aging of an Al-5 Zn-2 Mg alloy. The influence of aging treatment was examined for alloys with and without Ti addition. The alloys were solution heat treated at 510°C, air cooled then aged at various temperatures below the G.P. zone solvus for short times before aging above the G.P. zone solvus at 200°C. The Ti addition alloy yields a small precipitate free zone (PFZ $\sim 0.3\mu$) and a higher density of precipitate near the edge of the PFZ than in the mid-grain region. The ternary alloy without Ti addition produces a wide range of PFZs size (0.4 to 4μ) depending upon the aging temperature below the G.P. zone solvus. Significant changes in the morphology of the matrix precipitate, the amount of grain boundary precipitate, and the width of PFZ, were observed in single stage aging at 200°C as a result of the Ti addition. These results could be explained in terms of Ti interacting with vacancies or solute atoms, causing the changes in the vacancy and/or solute concentration profiles. A model based upon solute and vacancy concentrations coupled with a time at temperature effect has been developed to allow the interpretation of the observed two-stage aging results in an Al-Zn-Mg alloy.

ACCESSION FOR		
NTIS	White Section	<input checked="" type="checkbox"/>
DDC	Buff Section	<input type="checkbox"/>
UNANNOUNCED		<input type="checkbox"/>
JUSTIFICATION		
<i>Added on file</i>		
BY		
DISTRIBUTION/AVAILABILITY CODES		
DIST.	AVAIL.	and/or SPECIAL
A		

INTRODUCTION

Alloys based on the Al-Zn-Mg system have the highest strength of all the age-hardenable light alloys. One of the disadvantages of these alloys has been their susceptibility to stress corrosion cracking (SCC), a phenomenon undoubtedly related to the microstructure of the alloy. The majority of experiments to date have employed either heat treatment or alloying additions to alter the microstructures, which in turn, alters the SCC susceptibility.

Precipitation in Al-Zn-Mg alloys generally occurs in the sequence: Supersaturated Solid Solution \rightarrow G.P. Zones \rightarrow η' \rightarrow η (MgZn_2). An important characteristic of these aged alloys is the presence of precipitate free zones (PFZs). Thomas and Nutting¹, Taylor², and Embury and Nicholson³ suggested that the formation of the PFZ was the result of a critical vacancy concentration being required for precipitate nucleation. Later work by Unwin, Lorimer, and Nicholson⁴ observed that solute effects could be as important as vacancy effects in slow quenched specimens or specimens subjected to a quench interruption. According to the model of Lorimer and Nicholson⁵, on quenching from the solution heat treatment temperature, a vacancy concentration profile develops adjacent to the grain boundaries. Depending upon the time and temperature of aging at a temperature below the G.P. solvus, a size distribution of G.P. zones develops near the grain boundaries. When the temperature is raised above the G.P. solvus, zones with diameters greater than a certain critical diameter transform into precipitates. The edge of the PFZ occurs at

a distance from the boundary where all the G.P. zones have sizes less than the critical size. Unwin et al.⁴ suggested that the nature of grain boundary precipitation and the resulting solute profile should also be taken into account to completely characterize the nature of PFZs. It is clearly established that any model of PFZ formation should take into account the combined effects of solute profile and vacancy profile across grain boundaries.

Grove and Judd⁶ have reported that the width of PFZ, the extent of grain boundary precipitation, and the distribution of solute elements (Zn and Mg) of an Al-Zn-Mg alloy were observed to be affected by Ti additions.

The present work on Al-Zn-Mg and Al-Zn-Mg-Ti alloys was undertaken to obtain a better understanding of the role played by Ti on the precipitation process and the formation of PFZ. Previous models do not adequately explain the present results of the PFZ sizes obtained in two-stage aging treatments. A model based upon solute and vacancy concentrations coupled with a time at temperature effect has been developed to allow the interpretation of the observed two-stage aging results in an Al-Zn-Mg alloy.

EXPERIMENTS

i) Alloys

The alloys used in this investigation were (1) Alloy P: Al-5.18% Zn-1.79% Mg-0.13% Ti* and (2) Alloy Q: Al-5.06% Zn-1.97% Mg-0.007% Ti** by weight.

* Alloy P will be referred to as the Ti addition alloy

** Alloy Q will be referred to as the ternary Al-Zn-Mg alloy

High purity (99.99% or 99.9% pure) Al, Zn, Mg, and Ti were used to prepare the alloys. Alloy P was homogenized for one week at 580°C and Alloy Q for the same amount of time at 465°C. The alloys were then processed in ten stages by cold reduction and intermediate anneals to a thickness of 0.254 mm.

ii) Heat Treatment

All the samples used in this study were solution heat treated in a vertical tube air furnace at $510^{\circ}\text{C} \pm 3^{\circ}\text{C}$ for 3 hours and then quenched into the chosen quenching medium (brine at -10°C or air). Oil baths which were controlled to less than $\pm 2^{\circ}\text{C}$ were used for subsequent aging treatments. Single aging treatments for varying lengths of time were performed at 200°C . The G.P. zone solvus was estimated to be $\sim 150^{\circ}\text{C}$ ⁷. Two-stage aging treatments were performed at various temperatures (70, 105, 120, 135°C etc.) below the G.P. zone solvus for short times (5 and 20 min.) and then the samples were immediately up quenched in oil and aged at 200°C . At the completion of aging, the specimens were water quenched and stored in liquid nitrogen to prevent aging at room temperature.

iii) Electron Microscopy

Transmission electron microscopy was performed to determine the microstructures of the samples. Thin foils were prepared by jet-polishing employing an electrolyte of 80% methanol, 20% nitric acid. The electrolyte was maintained at a temperature of -10°C . A potential in the range of 10 to 15 volts was used for the thinning. The voltage employed depended upon the heat treatment conditions. Examination was performed with JEOL-100C Microscope operated at 100Kv.

iv) Measurements

a) Grain Boundary Precipitation

The measurements of grain boundary precipitation were made directly from the photomicrograph negatives from samples in which the plane of the grain boundary was essentially parallel to the incident electron beam. The fractional length of the boundary occupied by the precipitates, F , was calculated. The length and width of the grain boundary precipitates were also measured.

b) Precipitate-Free Zone Width

The measurement of PFZ width, W , was similar to the method used by Shastri and Judd⁸. The average PFZ width, \bar{W} , was calculated from the individual values of W (at least 3 measurements) in specimens of a given heat treatment.

In the case of a wide PFZ ($>2\mu$), the matrix precipitate is often scattered, rendering the above method unsuitable. For this purpose, two lines were drawn parallel to the grain boundary, one on each side, within which no more than 20 precipitates appeared in the photographs at magnification of 10,000 X. The distance between these two lines was then defined to be the width of the PFZ.

c) Matrix Precipitation

The density (# of ppts/cm²), D , of matrix precipitate was taken at the thinnest areas in the sample in the mid-grain regions away from the grain boundary. The matrix precipitate near the PFZ is usually different in some aspects of microstructural characterization from the mid-grain precipitate. The size of the precipitate was determined from the average of measurements on at least ten precipitates.

The foil thickness was assumed to be constant between specimens in the region used for measurements, since all specimens were all similarly prepared and observed. Any errors that might have been introduced in F and D due to the departure of foil thickness from the average value were assumed to be small.

RESULTS

i) Single-Stage Aging

The line fraction of grain boundary occupied by precipitate (F) and the length (L) and width (W) of grain boundary precipitate for air cooled specimens aged at 200°C for 0, 5, 30 and 240 minutes are shown in Table I. The as quenched structure of Ti addition alloy shows very little or no grain boundary precipitate. The line fraction of grain boundary occupied by precipitate (F) increased with aging time and the F value of the Ti addition alloy is less than that of the ternary alloy for each aging time at 200°C. The grain boundary precipitates of the Ti addition alloy are also smaller than for the ternary alloy. These results are in agreement with the earlier work of Grove and Judd⁶ in which they suggested that Ti retards the formation of solute-vacancy complexes which would then result in a reduction of the rate of formation of grain boundary precipitate.

Table II gives the width of the PFZ, the density and size of the matrix precipitate for brine quenched and air cooled specimens that were aged at 200°C for 4 hours. The width of the PFZ of the Ti addition alloy is smaller than that of the ternary alloy in both

air cooled and brine quenched specimens. Figure 1(a) and Figure 1(b) show the difference in the PFZ of the alloys which were brine quenched then aged at 200°C for 4 hours. The width of the PFZ increased by a factor of two for the Ti addition alloy and by a factor of five for the ternary alloy when the quench medium was changed from brine to air cooled. The difference in the morphology of the matrix precipitate in these alloys which were air cooled then aged at 200°C for 4 hours is shown in Figure 2(a) and in Figure 2(b).

ii) Two-Stage Aging

Alloys subjected to two-stage aging treatments are sensitive to the first aging treatment which affects the dispersion of the G.P. zones and the PFZ size. Table III summarizes the width of the PFZ, the density and size of the matrix precipitate of alloys that were air cooled followed by a two-stage aging treatment. For all these treatments, the Ti addition alloy produces very similar microstructures, with nearly the same width of PFZ ($\sim 0.3\mu$) and a higher density of precipitate near the edge of the PFZ than in the mid-grain. Figure 3(a) is a typical example of the microstructure in two-stage aging for the Ti addition alloy which was aged at 70°C for 5 min. then at 200°C for 1 hour. Figure 3(b) represents the same treatment as above but for the ternary. The ternary displays a relatively large PFZ and a lower density but larger precipitate at the edge of the PFZ than in the mid-grain. The variation of the average width of PFZs with first aging temperatures of these two alloys is shown in Figure 4. It is seen that a C shaped curve for the ternary alloy gives a

minimum PFZ at some intermediate first aging temperature. This phenomenon in two-stage aging will be discussed in detail in the next section. The density of matrix precipitate goes through a maximum at intermediate first aging temperatures in the alloys. The temperature corresponding to the maximum appears to be around 105°C for the alloys. It should be noted that the density of matrix precipitate of the Ti addition alloy is less than that of the ternary alloy in each aging treatment.

Table IV shows the effect of aging time of the first aging temperature on the PFZ. The density of matrix precipitate increased as the first aging time was prolonged. The width of the PFZ in the ternary alloy varies drastically from 2.5 μ to 0.17 μ as a function of heat treatment. This variation will be explained in the model proposed in the next section.

DISCUSSION

In recent years, the study of PFZs has evoked considerable theoretical interest because it has been suggested⁵ that the role of vacancy and solute supersaturations can be deduced from the microstructure of the PFZ. Two mechanisms have been proposed for the formation of PFZs⁹. (1) Vacancy-depletion mechanism. The excess vacancies in the region adjacent to the grain boundaries migrate to the grain boundaries which act as sinks for vacancies, causing a dearth of nucleation sites. (2) Solute-depletion mechanism. The grain boundary precipitates deplete the adjacent grain regions of solute

atoms and thereby lower the solute supersaturations. Hence precipitation is prevented in these regions. Thomas and Nutting¹ suggested the PFZs could be formed as a result of (1) vacancy depletion, (2) solute depletion, or (3) combination of both (1) and (2). Jacobs and Pashley¹⁰ took into account the variation in solute profiles adjacent to the grain boundary due to the heterogeneous precipitation at the grain boundaries and solute segregation during quenching.

i) Single-Stage Aging Treatment

It is generally believed that when aged above the G.P. solvus, the vacancy mechanism is adequate to explain the formation of PFZ¹¹. In cases where it was decided to minimize the contribution of depletion to the formation of PFZ, an aging temperature well above G.P. solvus was used, e.g. 200°C in this study. Grove and Judd⁶ have suggested that Ti prevents or lowers the likelihood of the formation of solute-vacancy complexes by either an interaction with vacancies or by a strong interaction with solute atoms. Doyama¹² found there is a relationship between vacancy-impurity binding energy and the solid solubility limit in Al. He suggested that in Al the Ti atoms are more strongly associated with vacancies than either the Mg or the Zn atoms. Figure 5 is the proposed vacancy concentration profile of the Ti addition alloy and of the ternary alloy which were quenched from solution temperature. Ti has an equilibrium constant, $k > 1$ in aluminum. Therefore, Ti tends to concentrate at the center of the grain¹³, and so the concentration

profile of Ti could be regarded as shown in Figure 6. Since the grain boundary is an ideal sink for vacancies coupled with the distribution and proposed behavior of the titanium present, the interaction between Ti and vacancies at near and intermediate distances increases with increasing distance from the grain boundary. This results in the relative maximum in the mobile vacancy concentration as shown in Figure 5. The high solute concentration at the grain boundary as shown in Figure 6 and 7 is due to the grain boundary precipitation and solute segregation during quenching.

There is much less Ti retardation of movement of vacancies in the ternary; more vacancies are annihilated by migration to grain boundaries. The mobile vacancy concentration which is important in the nucleation process near grain boundary regions is lowered. Assuming that the critical vacancy concentration required for precipitates nucleated at 200°C is the same for these alloys, then the intersections of concentration profiles and the horizontal dash line defined the regions of PFZs. The difference in the width of PFZs of the alloys as given in Table II can thus be explained. The density of matrix precipitate increased about 12 times for the ternary alloy and 2 times for the Ti addition alloy when changing the quench medium from air to brine. The brine quench results in a much higher density and the PFZ microstructure shows that the ternary alloy is more quench sensitive than the Ti addition alloy.

ii) Two-Stage Aging

a) Ternary Al-Zn-Mg Alloy

To interpret the results of the PFZs from two-stage aging treatments of the ternary alloy, it is necessary to use a model based upon both vacancy and solute effects. This is developed as follows. It is proposed, on quenching from the solution heat treatment temperature, the vacancy and solute concentration profiles develop adjacent to the grain boundary as shown in Figure 7. For a given short time at the first aging temperature which is below $T_{G.P.}$, there is a minimum combination of solute and vacancy concentration, C_V and C_S respectively, required for G.P. zones or precipitates which have reached the critical size for nucleation at 200°C. At the edge of the PFZ, the G.P. zones have the size corresponding to the critical diameter. For example, at an intermediate aging temperature (T_I), it means that a solute concentration (C_{SI}) and a vacancy concentration (C_{VI}) are needed in order to form G.P. zones or precipitates of the critical size for nucleation of stable precipitates at 200°C. At a high aging temperature (T_H), C_{SH} and C_{VH} are required to form precipitates of stable size at 200°C. C_{SL} and C_{VL} have the same meaning except at a low aging temperature (T_L). The higher the first aging temperature, the higher the solute concentration required, i.e., $C_{SH} > C_{SI} > C_{SL}$. The C-shaped curve in Figure 7 represents the boundaries of PFZs of various first aging temperature. On the left side of the curve is the regions of PFZs. The wide PFZ and low density of matrix precipitate at high first aging temperature as given in Table III

results from the fact that the stability of G.P. zones, solute and vacancy supersaturations are low. At low temperature, due to slow diffusion of solute atoms, the number of zones formed is less. Regardless of the fact that at low temperatures the solute and vacancy supersaturations are high, the density of precipitate is also low and the PFZ is wide. At high and low first aging temperatures, there are more vacancies required to meet the minimum combination of solute and vacancy concentration. At an intermediate temperature, reasonably high solute, vacancy supersaturations and diffusion rates result in a higher density of precipitates and a smaller PFZ than either high or low aging temperature. It is evident that the first aging treatment plays a very important role in the formation of the PFZ when a two-stage aging treatment is employed. The C-Curve in Figure 7 is a complex function of solution temperature, quench medium, aging time and temperature, $T_{G.P.}$, and alloy composition etc.

According to this model, changes in the time at first aging temperature and in the quench medium should affect the width of PFZ. Prolonged periods of time at first aging temperature of two-stage aging treatments would develop a smaller PFZ with time due to the fact that the longer time allows more G.P. zones and/or precipitates to form and grow. The positions relative to the grain boundary where G.P. zones or precipitates have reached critical size at 200°C would then move closer to the grain boundaries. Figure 4 shows the movement of the C-Curve to the grain boundary by increasing aging time from 5 min to 20 min. This movement is not uniform everywhere

so the shape of the C-Curve is changed as aging time increased. For example, as the aging time increased, the width of PFZs decreased from 1μ to 0.37μ and from 0.44μ to 0.36μ at the first aging temperature of 70°C and 105°C , respectively. If the first aging time is sufficiently long, the C-Curve in Figure 7 would become far less curved, to the point where the "C" nature could disappear. Since at low temperature, high solute and vacancy supersaturations would dominate the nucleation process, the resulting width of the PFZ would be narrow. Table V shows that the width of PFZ is greatly reduced from 2.2μ for air cooled to 0.61μ for brine quenched. This is due to the increase of vacancy concentration and the decrease of solute segregation to the grain boundary¹⁴ by increasing quench rate from air cooled to brine quenched. The brine quenched samples after being aged at 135°C for 5 min. followed by 1 hr at 200°C show both homogeneous and heterogeneous regions of precipitates.

b) Al-Zn-Mg-Ti Alloy

The proposed vacancy, solute (Zn+Mg), and Ti concentration profiles for the Ti addition alloy are shown in Figure 6. The vacancy and Ti concentration profiles have been described earlier. The solute concentration profile of Al-Zn-Mg as suggested by Doig and Edington¹⁵ is depicted in Figure 7. The addition of Ti to an Al-Zn-Mg alloy results in an interaction between Ti and solute atoms⁶. Since this interaction increases with increasing Ti concentration, the resultant mobile solute concentration profile would show a relative maximum, as seen in Figure 6. The size distribution of G.P. zones

after short time aging at a temperature below $T_{G.P.}$ is also indicated in the figure. On aging at 200°C , the density of precipitation increases near the edge of the PFZ (Figure 3a) both because of higher solute and vacancy concentrations as well as the presence of the more stable G.P. zones in that region. Thus the width of the PFZs in the Ti addition alloy subjected to two-stage aging treatments was confined to these regions. Figure 4 shows that the variation in the width of the PFZs of Ti addition alloy samples with first aging temperature below $T_{G.P.}$ for 5 min followed by 1 hr at 200°C is small and that the marked C-Curve is absent. When the samples were directly aged at 200°C for 1 hr without first being aged at a temperature below $T_{G.P.}$, there was a notable absence of a high density of precipitates near the PFZ edge, as seen in Figure 8. The density of precipitate decreases with increased distance away from the grain boundary in the two-stage aged Ti addition alloy (Aged 150°C for 5 min then at 200°C for 1 hr) as shown in Figure 9. This observation is opposite to that of the ternary alloy in which the density of precipitate increases with increased distance from the grain boundary. This phenomenon is in agreement with the proposed vacancy and solute concentration profiles of the Ti addition alloy.

The density of matrix precipitate was measured in regions away from PFZs. At these regions, mobile solute and vacancy concentrations would be lower for Alloy P than for Alloy Q for each two-stage aging treatment (Table III). This could be interpreted as Ti reducing the mobility of Zn and Mg^6 ; thus the number of G.P. zones or precipitates which form at aging below $T_{G.P.}$ having reached

the critical nucleation size at 200°C, is reduced. Nicholson¹⁶ reviewed the possible effects of trace element additions on the precipitation process in Al-Zn-Mg alloys. One of the effects is the change of the interface energy of G.P. zones or precipitates, e.g. Cd in Al-Cu alloys was absorbed at the interface with the precipitate, thereby lowering the interface energy. For non-coherent precipitates, the interface energy and the disregistry between matrix and precipitate are important factors to determine the morphology of the precipitate. The change of the Al lattice parameter per weight per cent Ti in the binary solid solution is -0.006\AA .¹⁷ Small additions of Ti to an Al-Zn-Mg alloy are therefore not expected to significantly vary the lattice parameters of the matrix and/or the precipitate. The change in the morphology of precipitates due to Ti addition implies the possible changes in the relative surface energy of crystal planes. The surface free energies of f.c.c. metals have been observed to vary by about 16% of the mean surface energy.¹⁸ The relative surface free energy of crystal planes might be lower in the ternary alloy than that in the Ti addition alloy.

CONCLUSIONS

1. A model explaining the width of precipitate-free zones as a function of two-stage aging treatments and alloying addition was developed. The proposed model was able to explain the observed PFZ microstructure in Al-Zn-Mg and Al-Zn-Mg-Ti alloys for numerous aging treatments and for PFZ widths varying as much as one order of magnitude. When plotted as a function of the first aging temperature, the observed PFZ width followed a C-shaped curve with the smallest width observed at an intermediate temperature (105°C) and wider PFZ widths at both higher and lower temperatures.

2. The Ti addition alloy produces very similar microstructures for all the first aging temperatures except at room temperature, with nearly the same width of PFZs ($\approx 0.3\mu$) and a higher density of precipitate near the edge of the PFZ than in the mid-grain of two-stage aging. The absence of the C-Curve for the Ti addition alloy could be explained in terms of Ti interacting with vacancies and solute atoms, causing the changes in concentration profiles.
3. The addition of Ti to an Al-Zn-Mg alloy reduced the amount of grain boundary precipitation and the width of precipitate free zone. It also changed the morphology of the matrix precipitate in the single aging treatment at 200°C .
4. The Ti addition alloy has less quench sensitivity than that of the ternary alloy. The width of PFZ decreased from 0.6μ to 0.3μ for the Ti addition alloy and from 4μ to 0.8μ for the ternary alloy. The density of the matrix precipitate increased approximately 2 times for the Ti addition alloy and 12 times for the ternary alloy when changing the quench medium from air cooled to brine quenched followed by aging at 200°C for 4 hr.

ACKNOWLEDGEMENTS

We gratefully acknowledge the support of the U. S. Office of Naval Research (Contract No. N00014-75-C-0504).

REFERENCES

1. G. Thomas and J. Nutting, J. Inst. Metals, Vol. 88, 1959-60, p. 81.
2. J. L. Taylor, J. Inst. Metals, Vol. 92, 1963-64, p. 301.
3. J. D. Embury and R. B. Nicholson, ACTA Met. Vol. 13, 1965, p. 403.
4. P. N. T. Unwin, G. W. Lorimer and R. B. Nicholson, ACTA Met. Vol. 17, 1969, p. 1363.
5. G. W. Lorimer and R. B. Nicholson, ACTA Met. Vol. 14, 1966, p. 1009.
6. C. A. Grove and G. Judd, Met. Trans, 4, 1973, p. 1023.
7. J. J. Polmear, J. Inst. Metals, Vol. 87, 1958-1959, p. 24.
8. C. R. Shastri and G. Judd, Met. Trans. Vol. 2, 1971, p. 3283.
9. E. A. Starke, Jr., J. Metals, Jan., 1970, p. 54.
10. M. H. Jacobs and D. W. Pashley, "The Factors Controlling the Width of Precipitate Free Zones at Grain Boundaries in Al-Zn", presented at the Symposium on the Mechanism of Phase Transformations in Crystalline Solids, Manchester, England, July 1968.
11. W. F. Smith and N. J. Grant, ASM Trans. Vol. 62, 1969, p. 724.
12. M. Doyama, Physics Letters, Vol. 21, No 4, June 1966, p. 395.
13. L. F. Mondolfo, Metals and Mater, 1971, Vol. 5, p. 95.
14. C. R. Shastri and G. Judd, Met. Trans. Vol. 3, April 1972, p. 779.
15. P. Doig and J. W. Edington, Met. Trans. Vol. 6A, No 4, 1975, p. 943.
16. R. B. Nicholson, J. Inst. Met., Vol. 95, 1967, p. 91.
17. Alcoa, Aluminum I, p. 399, Edited by Kent R. Van Horn, ASM, Metals Park Ohio, 1967.
18. B. E. Sundquist, ACTA Met. Vol. 12, Jan. 1964, p. 67.

TABLE CAPTIONS

- Table I The line fraction of grain boundary occupied by precipitate (F), the length (L), and the width (W) of grain boundary precipitate for air cooled specimens aged at 200°C for 0, 5, 30, and 240 minutes.
- Table II The width of PFZ, the density and the size of matrix precipitate for brine quenched and air cooled specimens that were aged at 200°C for 4 hours.
- Table III The width of PFZ, the density and the size of matrix precipitate of air cooled specimens which were aged at various temperatures below the G.P. zone solvus for 5 min., followed by 1 hour at 200°C.
- Table IV The variation of aging time of the first aging temperature on the PFZ, the density and the size of matrix precipitate.
- Table V The effect of changing quench medium on the width of PFZ, the density and the size of matrix precipitate of two-stage aging treatment of the ternary alloy.

TABLE I

GRAIN BOUNDARY PRECIPITATE

AGING TIME AT 200°C		P	Q
		<u>Al-5.18Zn-1.79Mg-0.13Ti</u>	<u>Al-5.06Zn-1.97Mg-0.007Ti</u>
0	F		0.14 ± 0.06
	L	-	426 ± 226 Å ^o
	W		112 ± 76 Å ^o
5 min	F	0.28 ± 0.05	0.33 ± 0.07
	L	760 ± 298 Å ^o	1052 ± 640 Å ^o
	W	218 ± 96	246 ± 72 Å ^o
30 min	F	0.40 ± 0.13	0.63 ± 0.19
	L	1260 ± 460 Å ^o	2366 ± 888 Å ^o
	W	266 ± 46 Å ^o	448 ± 116 Å ^o
240 min	F	0.59 ± 0.06	0.69 ± 0.09
	L	2130 ± 685 Å ^o	2580 ± 680 Å ^o
	W	545 ± 127 Å ^o	790 ± 170 Å ^o

F = LINE FRACTION OF G.B. OCCUPIED BY PPT

L and W: LENGTH AND WIDTH OF G.B. PPT

TABLE II

	510°C (3 hr)	+		510°C (3 hr)
			BRINE	A.C.
		+		+
			200°C (4 hr)	200°C (4 hr)
			P	Q
PFZ (Å)	3233 ± 258		8030 ± 460	6330 ± 230
				40760 ± 45000
MATRIX PPT				
D (#/cm ²)	2.2 x 10 ¹⁰		15 x 10 ¹⁰	1.2 x 10 ¹⁰
L (Å)	1160 ± 740		< 300	1020 ± 580
W (Å)	340 ± 120		< 300	260 ± 80
				460 ± 80

D = DENSITY

L = LENGTH

W = WIDTH

TABLE III

ALLOY P	70°C	105°C	120°C	135°C	150°C
PFZ (Å)	3162 ± 486	2703 ± 55	2850 ± 244	3133 ± 185	3040 ± 131
D (#/cm ²)	9.0 × 10 ⁹	3.4 × 10 ¹⁰	1.5 × 10 ¹⁰	1.5 × 10 ¹⁰	1.0 × 10 ⁹
L (Å)	160 ± 30	290 ± 100	320 ± 140	330 ± 140	330 ± 110
W (Å)	120 ± 20	150 ± 40	150 ± 50	170 ± 50	140 ± 60

ALLOY Q	10100 ± 270	4400 ± 260	4275 ± 269	22100 ± 4500	42800 ± 8500
PFZ (Å)	10100 ± 270	4400 ± 260	4275 ± 269	22100 ± 4500	42800 ± 8500
D (#/cm ²)	2.3 × 10 ¹⁰	7.8 × 10 ¹⁰	5.9 × 10 ¹⁰	4.5 × 10 ¹⁰	1.3 × 10 ¹⁰
L (Å)	340 ± 170	220 ± 90	310 ± 150	320 ± 100	320 ± 110
W (Å)	150 ± 50	100 ± 50	140 ± 40	130 ± 50	160 ± 40

ALL SAMPLES WERE SOLUTION HEAT TREATED AT 510°C FOR 3 HOURS, AIR COOLED, THEN AGED AT VARIOUS TEMPERATURES BELOW THE G.P. SOLVUS FOR 5 MINUTES, FOLLOWED BY 1 HOUR AT 200°C.

TABLE IV

HEAT TREATMENT

ALLOY P	A	B	C	C
PFZ ($\overset{\circ}{\text{A}}$)	2063 ± 102	1746 ± 110	3040 ± 131	2307 ± 200
D ($\#/\text{cm}^2$) $\times 10^{10}$	1.2	8.0	0.56	1.8
L ($\overset{\circ}{\text{A}}$)	570 ± 320	210 ± 80	330 ± 110	360 ± 160
W ($\overset{\circ}{\text{A}}$)	210 ± 60	90 ± 30	140 ± 60	160 ± 60

ALLOY Q				
PFZ ($\overset{\circ}{\text{A}}$)	25260 ± 4680	1716 ± 78	42800 ± 8500	34690 ± 2930
D ($\#/\text{cm}^2$) $\times 10^{10}$	0.96	6.0	1.3	2.3
L ($\overset{\circ}{\text{A}}$)	640 ± 350	320 ± 200	320 ± 110	290 ± 150
W ($\overset{\circ}{\text{A}}$)	260 ± 120	130 ± 40	160 ± 40	160 ± 40

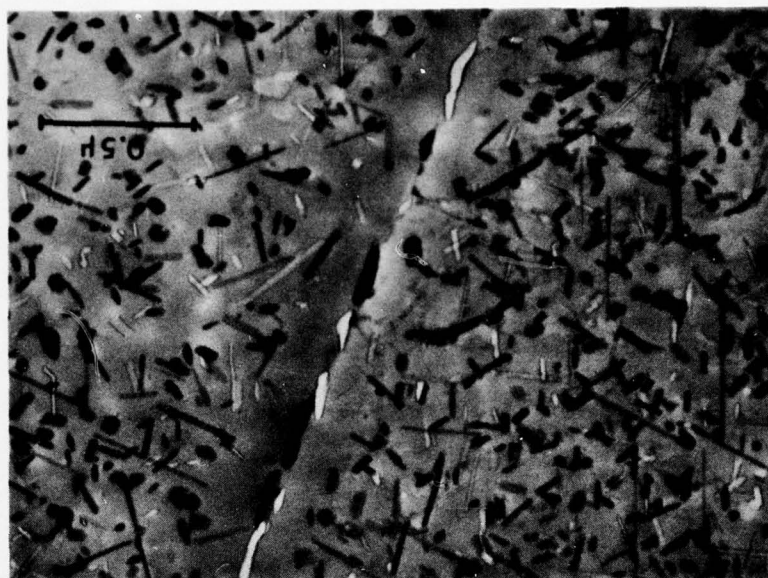
HEAT TREATMENT:

- (A) 510°C (3h) \rightarrow A.C. \rightarrow 135°C (5 min) \rightarrow 200°C (2h)
 (B) 510°C (3h) \rightarrow A.C. \rightarrow 135°C (1h) \rightarrow 200°C (2h)
 (C) 510°C (3h) \rightarrow A.C. \rightarrow 150°C (5 min) \rightarrow 200°C (1h)
 (D) 510°C (3h) \rightarrow A.C. \rightarrow 150°C (20 min) \rightarrow 200°C (1h)

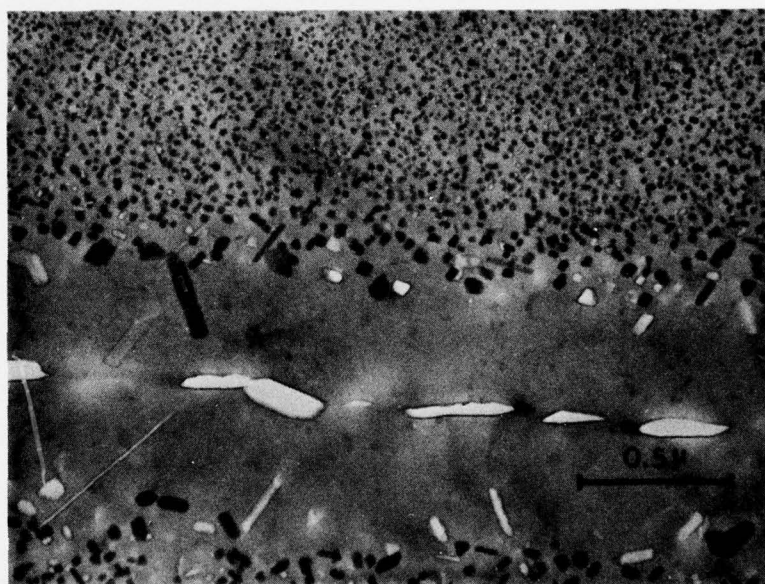
TABLE V

ALLOY Q - Al-5.06Zn-1.97Mg-0.007Ti

510°C (3 hr)	510°C (3 hr)
↓	↓
A.C.	BRINE (-10°C)
↓	↓
135°C (5 min)	135°C (5 min)
↓	↓
200°C (1 hr)	200°C (1 hr)
<hr/>	
PFZ (Å) $\sim 22,100$	~ 6100 In some G.B.'s, due to heterogeneous nucleation, PFZ is not clearly defined.
MATRIX PPT	
$D(\#/cm^2) \ 4.5 \times 10^{10}$	$> 20 \times 10^{10}$ for homogeneous regions
$L(\text{Å}) \ 320 \pm 100$	homogeneous region > 120 Å in diameter
$W(\text{Å}) \ 130 \pm 50$	heterogeneous region - needle-like > 1000 Å in length ~ 100 Å in width

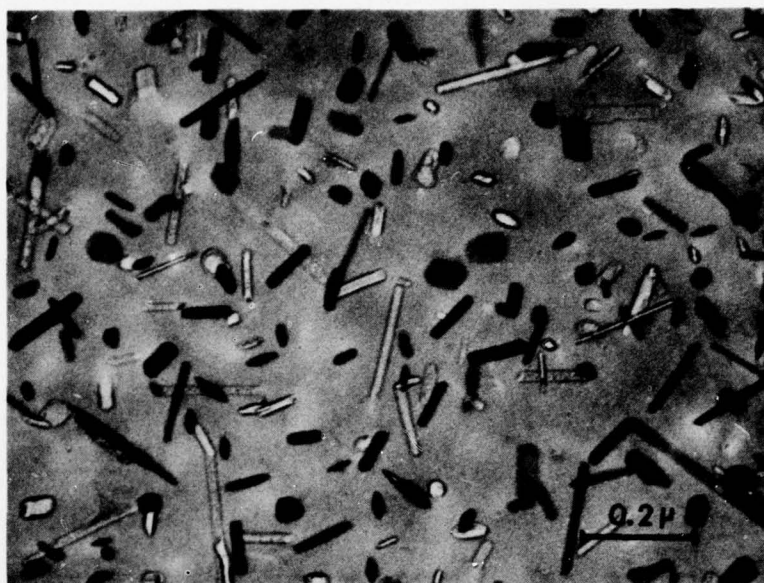


(a)

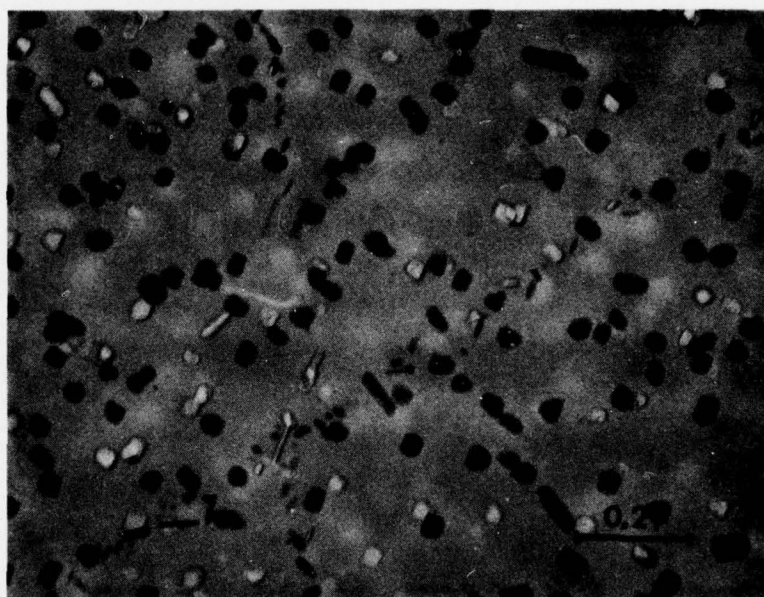


(b)

Fig. 1 The difference in PFZ of the alloys which were brine quenched then aged at 200°C for 4 hours; (a) the Ti addition alloy, (b) the ternary alloy.



(a)

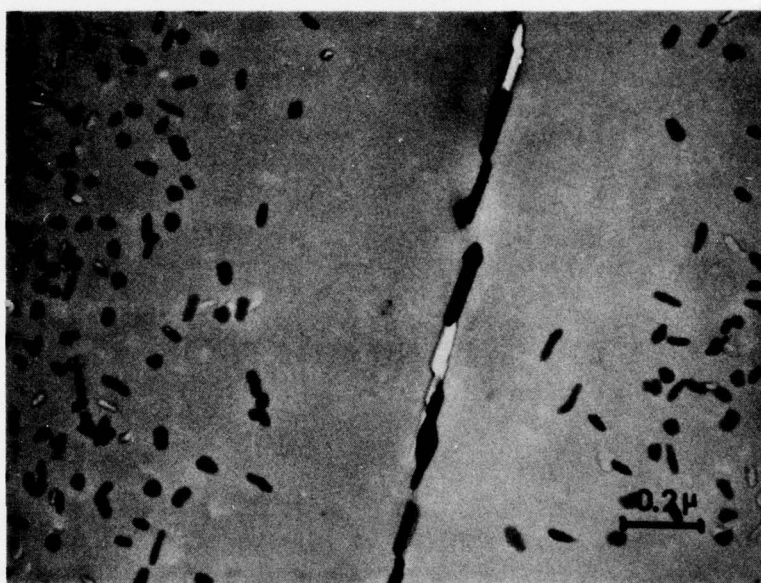


(b)

Fig. 2 The morphology of matrix precipitate in (a) the Ti addition alloy and (b) the ternary alloy which were air cooled then aged at 200°C for 4 hours.



(a)



(b)

Fig. 3 (a) Typical example of the microstructure in two-stage aging for the Ti addition alloy which was air cooled then aged at 70°C for 5 min. followed by 1 hour at 200°C; (b) the same treatment as (a) but for the ternary alloy.

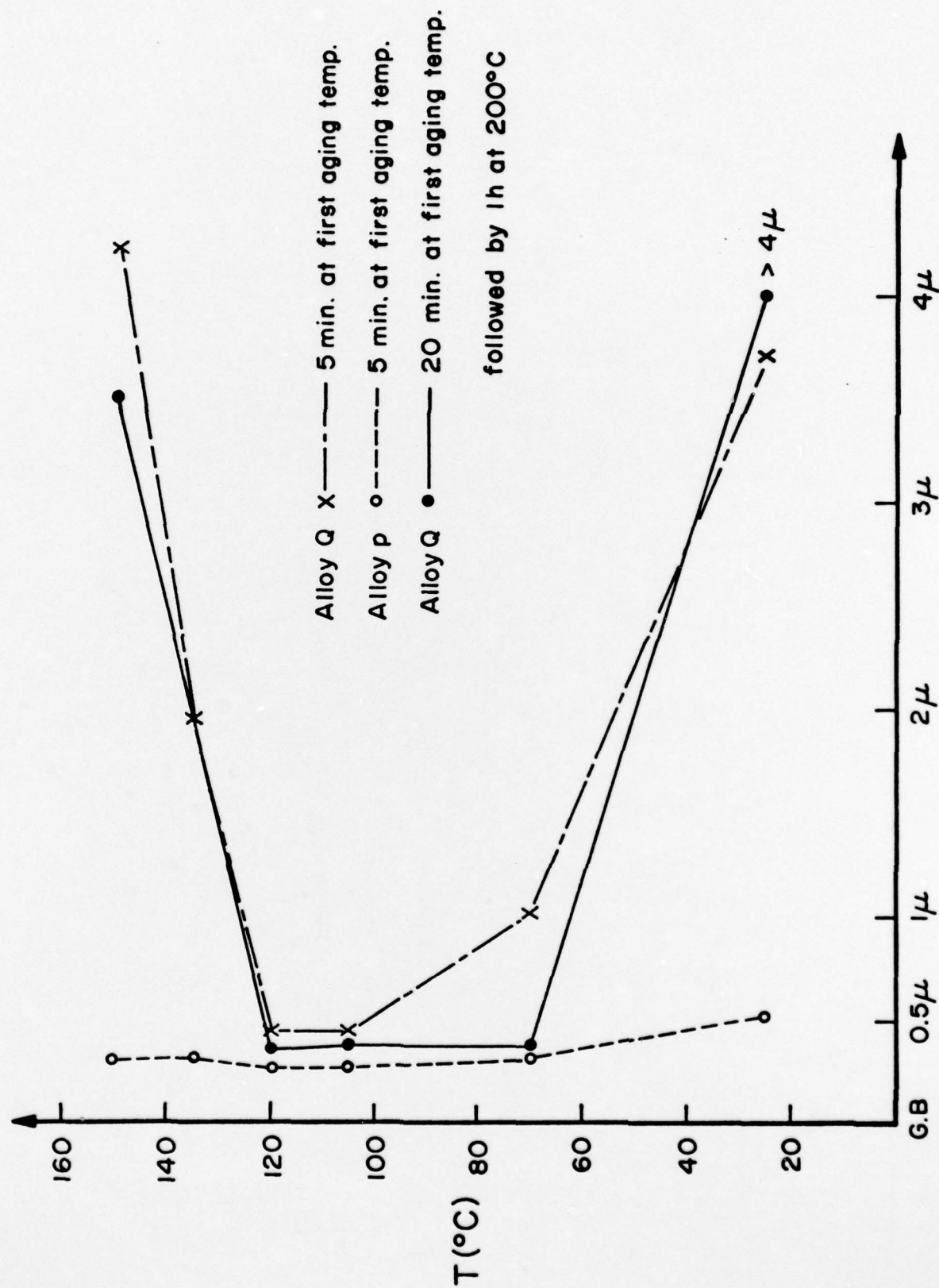


Fig. 4 The variation of the average width of the PFZs with first aging temperature of the Ti addition alloy and the ternary alloy.

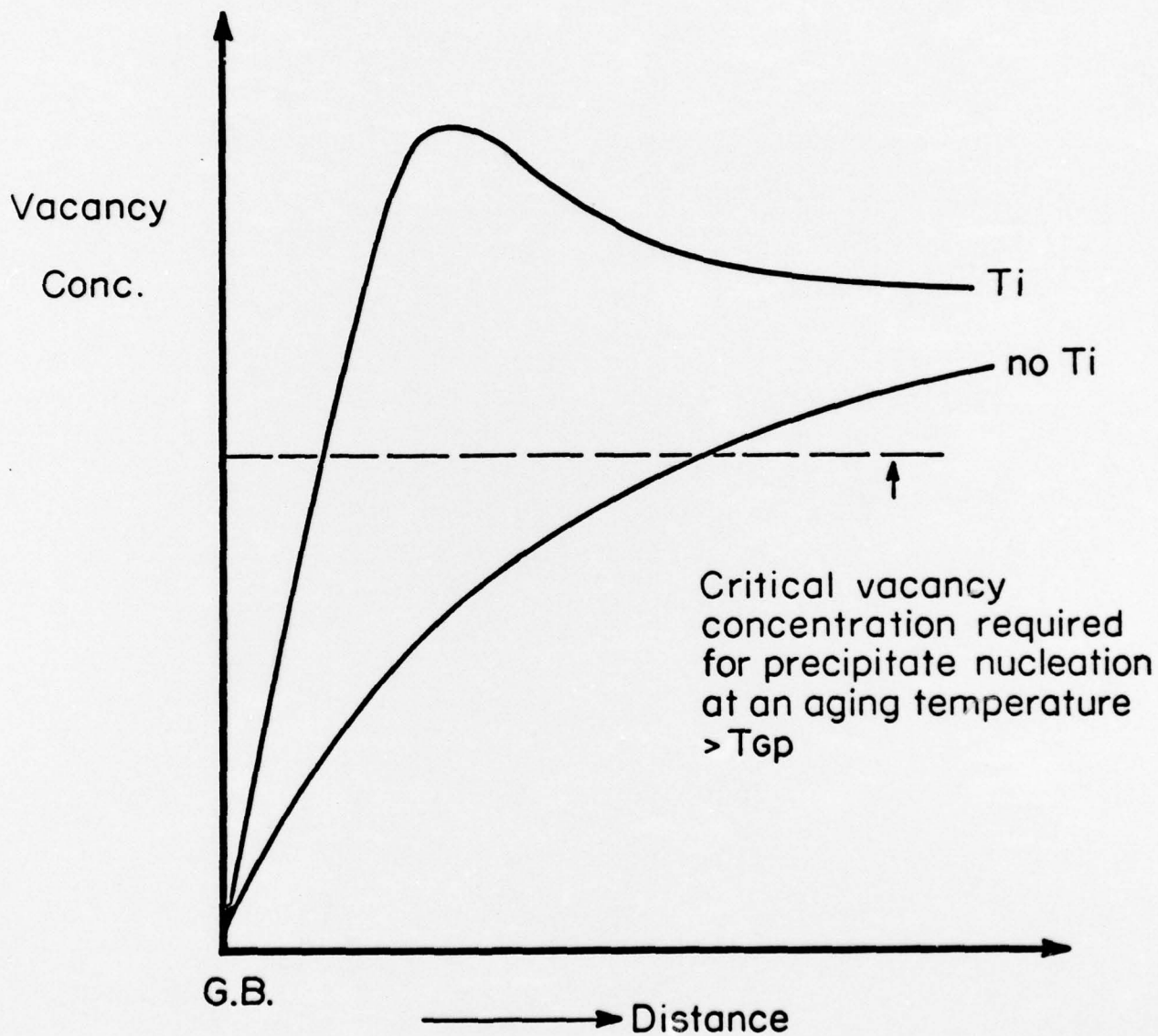


Fig. 5 The proposed vacancy concentration profile of the Ti addition alloy (Alloy P) and of the ternary alloy (Alloy Q) which were quenched from solution temperature.

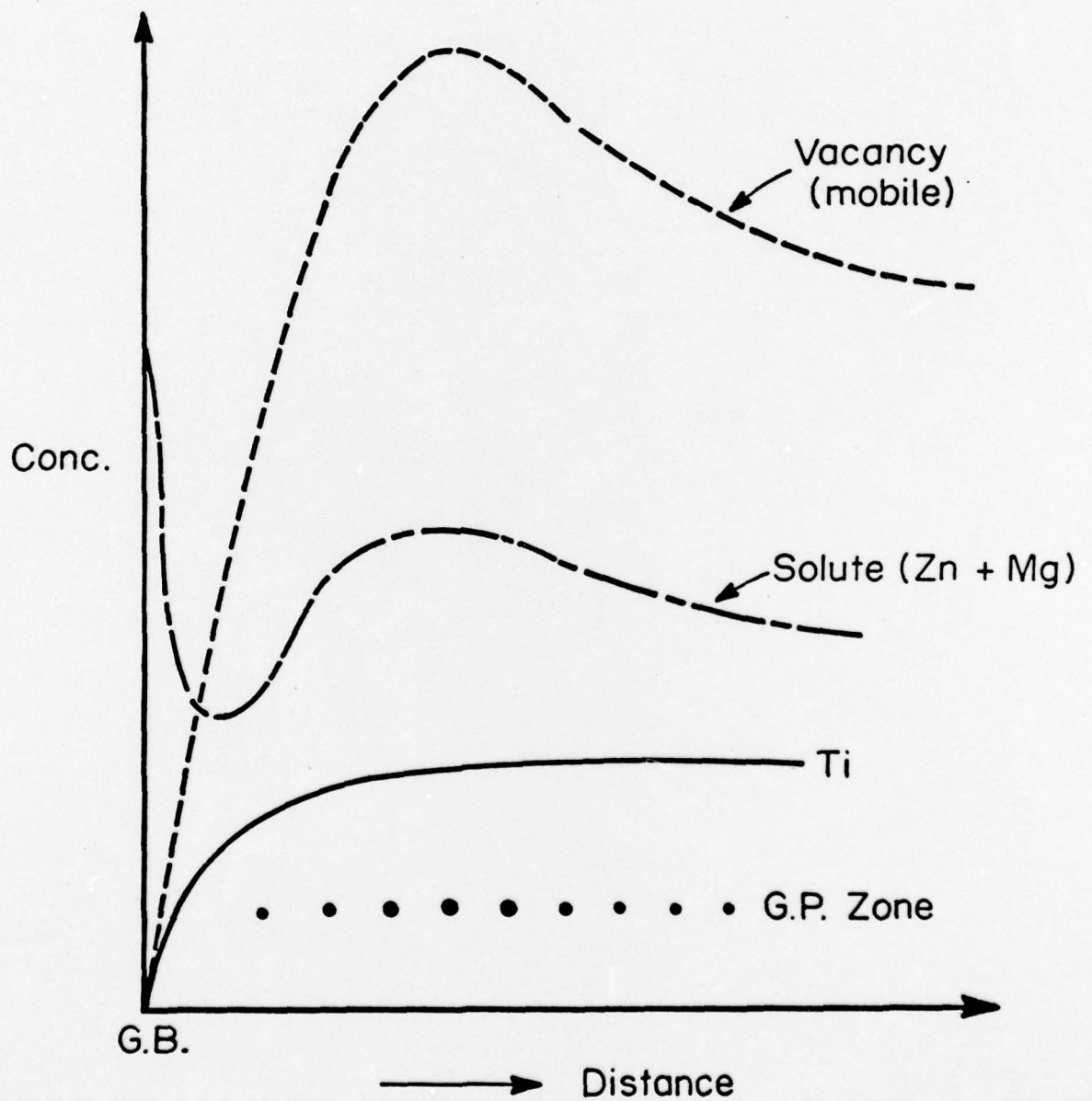


Fig. 6 The proposed vacancy, solute, and Ti concentration profiles for the Ti addition alloy.

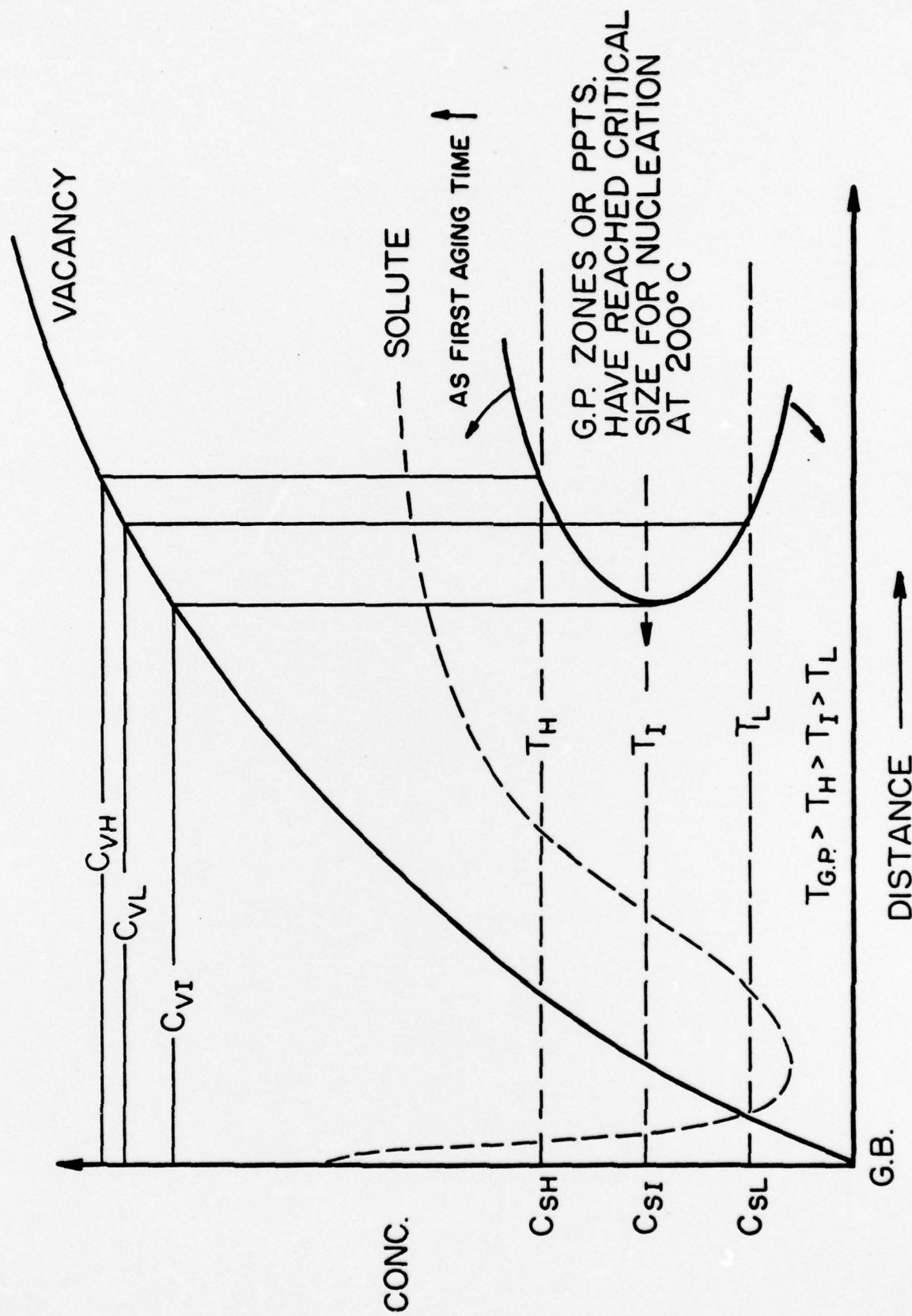


Fig. 7 A model of PFZ size based upon the vacancy and solute segregation to the grain boundary, the combination of vacancy and solute concentration required to form stable size at 200°C coupled with the effects of time and diffusion of solute atoms. The PFZ size corresponds to the curve showing the position of G.P. zones that have reached critical size.

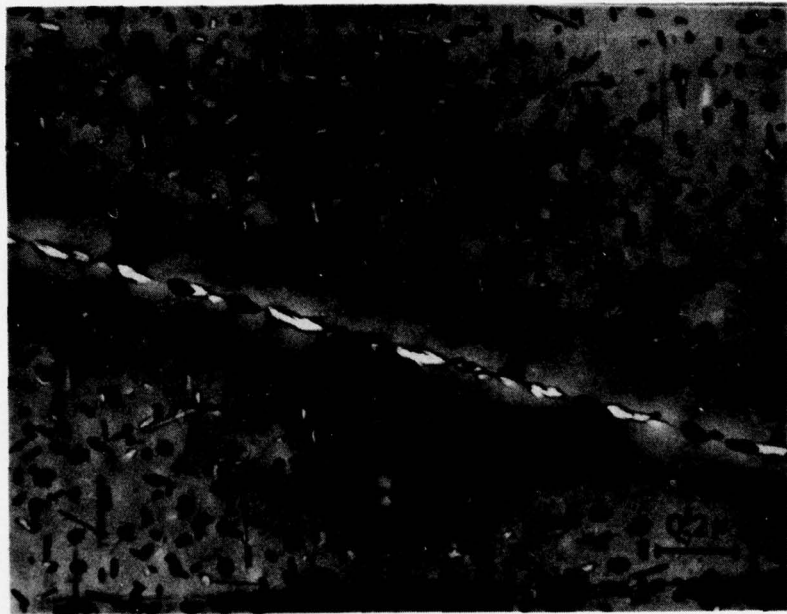


Fig. 8 The microstructure of the Ti addition alloy.
The specimens were aged at 200°C for 1 hr
without being aged at a temperature below $T_{G.P.}$



Fig. 9 The density of precipitate decreases with increased distance away from the grain boundary of the two-stage aged Ti addition alloy (aged at 150°C for 5 min. then at 200°C for 1 hr).